PERGAMON

International Journal of Solids and Structures 38 (2001) 5045–5062

INTERNATIONAL JOURNAL OF SOLIDS and STRUCTURES

www.elsevier.com/locate/ijsolstr

# A higher-order sandwich plate theory accounting for 3-D stresses

P. Frank Pai [a,*], Anthony N. Palazotto [b]

[a] *Department of Mechanical and Aerospace Engineering, University of Missouri-Columbia, E2403C Engineering Bldg. East, Columbia, MO 65211, USA*

[b] *Department of Aeronautics and Astronautics, Air Force Institute of Technology, Dayton, OH 45433, USA*

Received 2 August 2000

**Abstract**

In this paper we extend a layerwise higher-order shear-deformation theory to model a sandwich plate impacting with an elastic foundation at a low velocity. A new concept of sublaminates is introduced, and the new sandwich plate theory satisfies the continuity conditions of interlaminar shear and normal stresses, accommodates the normal and shear stresses on the bonding surfaces, and accounts for non-uniform distributions of transverse shear stresses in each layer. Moreover, the use of sublaminates enables the modeling of shear warpings that change with the spatial location, vibration frequency, and loading and boundary conditions. A finite-element model based on this sandwich plate theory is derived for performing direct transient analyses to predict the initiation and location of critical matrix crack and the threshold of impact damage. Moreover, analytical shear warping functions, shear coupling functions, and normal strain functions due to in-plane stretching, bending, transverse shearing, and surface loading are presented. 

*Keywords:* Sandwich plate theory; 3-D stresses; Sublaminates

## 1. Introduction

Sandwich structures have long been recognized as one of the most weight efficient plate or shell constructions for resisting bending loads. The aerospace industry, with its many bending stiffness dominated low-weight structures, has employed sandwich construction using aluminum honeycomb cores extensively. The most common currently fielded sandwich construction suffers from two major maintenance problems: corrosion damage to the core from trapped moisture, and low-velocity impact damage. The core corrosion problem can be greatly reduced by using a non-corrosive core such as Nomax honeycomb. Prediction of low-velocity impact damage to such structures is the subject of the present research. Low-velocity implies that the material properties can be assumed to be independent of strain rates. The failure modes commonly observed in composite sandwich plates subjected to low-velocity impact are fiber failure, matrix cracking,

* Corresponding author. Tel.: +1-573-884-1474; fax: +1-573-884-5090.
*E-mail address:* paip@missouri.edu (P.F. Pai).

0020-7683/01/$ - see front matter 
PII: S0020-7683(00)00356-5

delamination, and core crushing (Harrington, 1994), which are mainly caused by severe and complex three-dimensional (3-D) stress states.

Many of the current military and commercial applications of composite materials call for thick-section laminates composed of over 100 layers or sandwich panels with a honeycomb core between two face sheets of laminated composites. A primary concern in the analysis of thick-section laminates and sandwich panels is that transverse shear and normal stresses and deformations may not be negligible. Moreover, it is well known that low-velocity impact on a composite laminate can cause significant internal matrix cracks, delamination, and reduction in strength and stiffness. Experimental results in the literature show that initial impact damage is primary associated with matrix cracking and delamination is usually accompanied by a critical matrix crack (Choi et al., 1991). To predict the delamination and matrix cracking of composite laminates subjected to impact, an accurate estimation of transverse normal and shear stresses plays the key role in analysis.

For isotropic plates, transverse shear stresses $\sigma_{13}$ and $\sigma_{23}$ can be obtained from elasticity solutions as (Shames and Dym, 1985)

$$\sigma_{13} = G\gamma_5\left(1 - \frac{4z^2}{h^2}\right), \qquad \sigma_{23} = G\gamma_4\left(1 - \frac{4z^2}{h^2}\right)$$

Here $G$ is the shear modulus, $h$ is the thickness, $z$ is the thickness coordinate, and $\gamma_4$ and $\gamma_5$ are shear rotation angles on the reference plane $xy$. We note that this form of $\sigma_{13}$ is valid only if the $y$-axis represents the neutral axis of the crosssection on the $yz$ plane, and the form of $\sigma_{23}$ is valid only if the $x$-axis represents the neutral axis of the crosssection on the $xz$ plane. For an anisotropic laminate, the neutral axis of the crosssection on the $xz$ plane may not be on the midplane, the neutral axis of the crosssection on the $yz$ plane may not be on the midplane, and these two neutral axes may not be on the same plane. These cause difficulties in and reveal complexity of the analysis of anisotropic laminates. However, for symmetric and skew-symmetric laminates, the neutral axes are always on the midplane.

For a simply supported isotropic beam subjected to a uniformly distributed transverse load, Shames and Dym (1985) showed that $\sigma_{13}/\sigma_{11}$ is proportional to $h/L$ and $\sigma_{33}/\sigma_{11}$ is proportional to $(h/L)^2$, where $\sigma_{11}$ is the axial stress due to bending, $L$ the beam length, and $h$ the thickness. Hence, the transverse normal stress $\sigma_{33}$ is usually neglected and the transverse shear stresses are sometimes neglected in the analysis of thin-walled structures. However, transverse shear and normal stresses can be significant in thick composite laminates because of non-uniform distributions of external loads, elastic moduli, and Poisson's ratios.

In analyzing thick sandwich plates many researchers use 3-D finite elements, which are computational expensive. Some other researchers use predictor-corrector approaches, which use a classical laminate theory to predict the global response and then use 3-D elasticity equations to correct the predicted stresses for failure analysis. In this approach, the major questionable assumption is the rough modeling or negligence of interlaminar shear stresses. Hence, it is highly desirable to have a model that can capture the important 3-D effects due to through-thickness variations of displacements and stresses in thick laminates but maintain the efficiency and convenience of a 2-D model.

Two approaches have been taken in the development of laminate theories that incorporate higher-order effects in thick laminates; they are the equivalent single-layer approach and the discrete-layer approach. In equivalent single-layer theories, high-order terms are maintained in the expansion of the displacement components in the thickness coordinate (e.g., Savoia and Reddy, 1992). In this way, non-linear variations of displacements, strains, and stresses through the thickness of the laminate are permitted along with an approximation of transverse normal deformations and/or transverse shear deformations. These theories all provide improvements over the first-order shear-deformation theory but also have a common drawback. The thickness variation of displacements, and thus strains, is assumed to be continuous and smooth. This characteristic precludes the satisfaction of transverse stress continuity at interfaces between adjacent layers

of different materials and does not accurately reflect the kinematics in laminates that contain adjacent plies with drastically different constitutive properties. To overcome the drawbacks of equivalent single-layer theories, layerwise theories have been developed in which a unique displacement field is assumed within each layer. Theories of this type may be classified into two groups according to whether or not the number of degrees of freedom (DOFs) in the theory is dependent on the number of layers in the laminate. When the number of DOFs is coupled to the number of layers, the computational effort required in the analysis of thick laminates is comparable to that required by a fully 3-D analysis (Barbero et al., 1990). A few discrete-layer theories have been developed that contain a constant number of DOFs irrespective of the number of layers in the laminate (Bhimaraddi, 1995; Pai, 1995). In these theories, the additional DOFs are eliminated by enforcing continuity of transverse shear stresses at the interface of each two adjacent layers and by satisfying the zero shear traction conditions on the top and bottom surfaces of the laminate.

Comparison with results from 3-D continuum-based theories reveals that discrete-layer theories with a constant number of DOFs provide accurate approximations of structural response as well as through-thickness variations of in-plane displacements and stresses for composite laminates if the number of layers is not too large. However, it has been found that as the number of layers in the laminate and/or the complexity of the lamination scheme is increased, errors may increase to unacceptable levels.

In this paper we improve the layerwise higher-order shear-deformation theory of Pai et al. (1993) and Pai and Palazotto (1995) for modeling thick sandwich plates by introducing the concept of sublaminates and accounting for the transverse normal stress.

## 2. Sandwich plate theory

Fig. 1 shows the sandwich plate under investigation with its construction, loading conditions, and the coordinate system used. To include transverse shear deformations in the modeling of a general anisotropic laminated plate, each layer needs an assumed displacement field because of material non-uniformity through the laminate thickness. To account for transverse normal and shear stresses, we modify the layerwise third-order shear-deformation theory of Pai et al. (1993). In Fig. 1, $xyz$ is the reference coordinate system, $xy$ represents the reference plane of the laminate, $x$ and $y$ are in-plane coordinates, and $z$ is the thickness coordinate. We introduce here the concept of sublaminates to improve the accuracy in predicting transverse shear strains by using more dependent variables. A composite laminate will be divided into $M$ sublaminates. The $m$th sublaminate has $N_m$ layers and two shear rotation angles $\gamma_4^{(m)}$ and $\gamma_5^{(m)}$ at the $xy$ plane, as shown in Fig. 2. For the $i$th layer of the $m$th sublaminate, the displacement field is assumed to be

$$\begin{aligned} u_1^{(m,i)} &= u - w_x z + \gamma_5^{(m)} z + \alpha_1^{(m,i)} z^2 + \beta_1^{(m,i)} z^3 \\ u_2^{(m,i)} &= v - w_y z + \gamma_4^{(m)} z + \alpha_2^{(m,i)} z^2 + \beta_2^{(m,i)} z^3 \\ u_3^{(m,i)} &= w + \alpha_3^{(m,i)} z + \beta_3^{(m,i)} z^2 \end{aligned} \tag{1}$$

Here, $u(x,y,t)$, $v(x,y,t)$, and $w(x,y,t)$ are the displacements of the point on the $xy$ plane, $t$ denotes the time, $\alpha_1^{(m,i)}(x,y,t)$ and $\beta_1^{(m,i)}(x,y,t)$ account for the displacement along the $x$-direction due to shear warping, $\alpha_2^{(m,i)}(x,y,t)$ and $\beta_2^{(m,i)}(x,y,t)$ account for the displacement along the $y$-direction due to shear warping, and $\alpha_3^{(m,i)}(x,y,t)$ and $\beta_3^{(m,i)}(x,y,t)$ account for the variation of transverse normal displacement due to thickness change. Moreover, $(\ )_x \equiv \partial(\ )/\partial x$ and $(\ )_y \equiv \partial(\ )/\partial y$.

The constants $\alpha_1^{(m,i)}$, $\beta_1^{(m,i)}$, $\alpha_2^{(m,i)}$, and $\beta_2^{(m,i)}$ can be determined using the continuity conditions of inplane displacements and interlaminar shear stresses and the free shear stress conditions on the top and bottom surfaces of the laminate as shown next in Section 2.1. Moreover, the constants $\alpha_3^{(m,i)}$ and $\beta_3^{(m,i)}$ can be

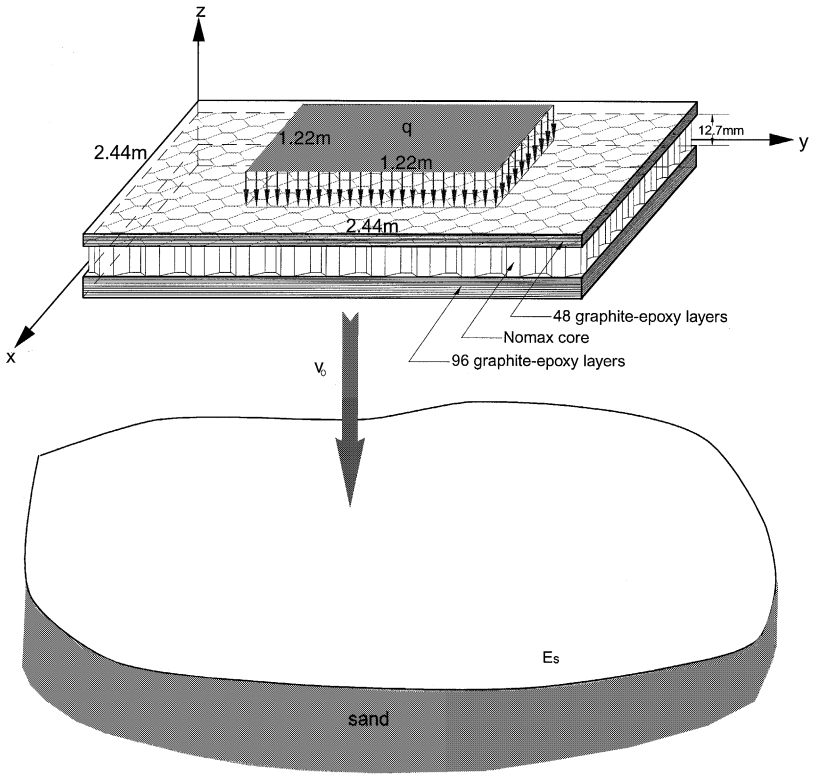


Fig. 1. The loadings, coordinates, and geometry of a sandwich plate impacting with an elastic foundation.

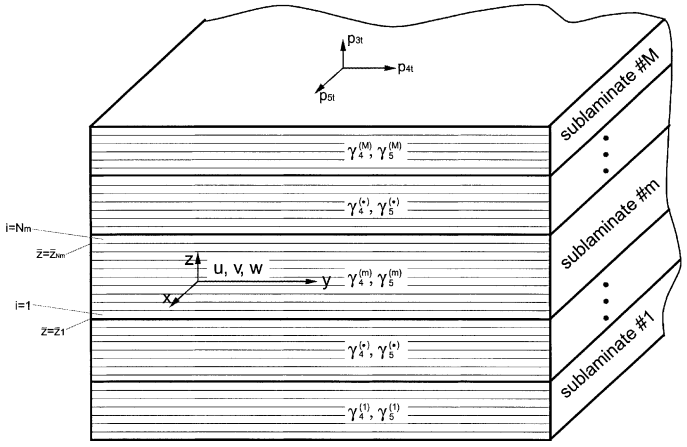


Fig. 2. The definitions of sublaminates and dependent variables.

determined using the continuity conditions of the transverse normal displacement and stress and the normal stress conditions on the top and bottom surfaces of the laminate as shown in Section 2.2.

It follows from Eq. (1) that the transverse shear strains of the $i$th layer of the $m$th sublaminate are

$$\begin{aligned}\epsilon_{13}^{(m,i)} &= \gamma_5^{(m)} + 2z\alpha_1^{(m,i)} + 3z^2\beta_1^{(m,i)} \\ \epsilon_{23}^{(m,i)} &= \gamma_4^{(m)} + 2z\alpha_2^{(m,i)} + 3z^2\beta_2^{(m,i)}\end{aligned} \tag{2}$$

Because the thickness change has no significant influence on transverse shear strains (Pai and Palazotto, 1995), we neglect $\alpha_3^{(m,i)}$ and $\beta_3^{(m,i)}$ in $\epsilon_{13}^{(m,i)}$ and $\epsilon_{23}^{(m,i)}$.

Using tensor transformations, one can obtain the transformed stiffness matrix $[\overline{Q}^{(m,i)}]$ for the $i$th layer of the $m$th sublaminate from its principal stiffness matrix $[Q^{(m,i)}]$ and its ply angle (measured with respect to the $x$-axis), and the stress–strain relations are given by (Whitney, 1987)

$$\left\{\sigma_1^{(m,i)}\right\} = \left[\overline{Q}_1^{(m,i)}\right]\left\{\epsilon_1^{(m,i)}\right\}, \qquad \left\{\sigma_2^{(m,i)}\right\} = \left[\overline{Q}_2^{(m,i)}\right]\left\{\epsilon_2^{(m,i)}\right\} \tag{3}$$

where

$$\begin{aligned}&\left\{\sigma_1^{(m,i)}\right\} = \left\{\sigma_{11}^{(m,i)}, \sigma_{22}^{(m,i)}, \sigma_{33}^{(m,i)}, \sigma_{12}^{(m,i)}\right\}^{\mathrm{T}}, \qquad \left\{\sigma_2^{(m,i)}\right\} = \left\{\sigma_{23}^{(m,i)}, \sigma_{13}^{(m,i)}\right\}^{\mathrm{T}} \\ &\left\{\epsilon_1^{(m,i)}\right\} = \left\{\epsilon_{11}^{(m,i)}, \epsilon_{22}^{(m,i)}, \epsilon_{33}^{(m,i)}, \epsilon_{12}^{(m,i)}\right\}^{\mathrm{T}}, \qquad \left\{\epsilon_2^{(m,i)}\right\} = \left\{\epsilon_{23}^{(m,i)}, \epsilon_{13}^{(m,i)}\right\}^{\mathrm{T}} \\ &\left[\overline{Q}_1^{(m,i)}\right] \equiv \begin{bmatrix} \overline{Q}_{11}^{(m,i)} & \overline{Q}_{12}^{(m,i)} & \overline{Q}_{13}^{(m,i)} & \overline{Q}_{16}^{(m,i)} \\ \overline{Q}_{12}^{(m,i)} & \overline{Q}_{22}^{(m,i)} & \overline{Q}_{23}^{(m,i)} & \overline{Q}_{26}^{(m,i)} \\ \overline{Q}_{13}^{(m,i)} & \overline{Q}_{23}^{(m,i)} & \overline{Q}_{33}^{(m,i)} & \overline{Q}_{36}^{(m,i)} \\ \overline{Q}_{16}^{(m,i)} & \overline{Q}_{26}^{(m,i)} & \overline{Q}_{36}^{(m,i)} & \overline{Q}_{66}^{(m,i)} \end{bmatrix}, \qquad \left[\overline{Q}_2^{(m,i)}\right] \equiv \begin{bmatrix} \overline{Q}_{44}^{(m,i)} & \overline{Q}_{45}^{(m,i)} \\ \overline{Q}_{45}^{(m,i)} & \overline{Q}_{55}^{(m,i)} \end{bmatrix}\end{aligned} \tag{4}$$

### 2.1. Shear warping functions

If there is no delamination, the in-plane displacements $u_1$ and $u_2$ and interlaminar shear stresses $\sigma_{13}$ and $\sigma_{23}$ are continuous across the interface of any two adjacent layers. Moreover, $\sigma_{23} = p_{4b}$ and $\sigma_{13} = p_{5b}$ at the bottom surface (i.e., $z = z_1$ of the first sublaminate) and $\sigma_{23} = p_{4t}$ and $\sigma_{13} = p_{5t}$ at the top surface (i.e., $z = z_{N_M+1}$ of the last sublaminate ), where $p_{4t}$ and $p_{5t}$ denote the shear loadings on the top surface of the laminate and $p_{4b}$ and $p_{5b}$ the shear loadings on the bottom surface of the laminate. Hence, we have

$$\begin{aligned}&\sigma_{23}^{(M,N_M)}(x,y,z_{N_M+1},t) - p_{4t} = 0 \\ &\sigma_{13}^{(M,N_M)}(x,y,z_{N_M+1},t) - p_{5t} = 0 \\ &u_1^{(m,N_m)}(x,y,z_{N_m+1},t) - u_1^{(m+1,1)}(x,y,z_1,t) = 0 \quad \text{for} \quad m = 1,\ldots,M-1 \\ &u_2^{(m,N_m)}(x,y,z_{N_m+1},t) - u_2^{(m+1,1)}(x,y,z_1,t) = 0 \quad \text{for} \quad m = 1,\ldots,M-1 \\ &\sigma_{23}^{(m,N_m)}(x,y,z_{N_m+1},t) - \sigma_{23}^{(m+1,1)}(x,y,z_1,t) = 0 \quad \text{for} \quad m = 1,\ldots,M-1 \\ &\sigma_{13}^{(m,N_m)}(x,y,z_{N_m+1},t) - \sigma_{13}^{(m+1,1)}(x,y,z_1,t) = 0 \quad \text{for} \quad m = 1,\ldots,M-1 \\ &u_1^{(m,i)}(x,y,z_{i+1},t) - u_1^{(m,i+1)}(x,y,z_{i+1},t) = 0 \quad \text{for} \quad i = 1,\ldots,N_m-1,\ m = 1,\ldots,M \\ &u_2^{(m,i)}(x,y,z_{i+1},t) - u_2^{(m,i+1)}(x,y,z_{i+1},t) = 0 \quad \text{for} \quad i = 1,\ldots,N_m-1,\ m = 1,\ldots,M \\ &\sigma_{23}^{(m,i)}(x,y,z_{i+1},t) - \sigma_{23}^{(m,i+1)}(x,y,z_{i+1},t) = 0 \quad \text{for} \quad i = 1,\ldots,N_m-1,\ m = 1,\ldots,M \\ &\sigma_{13}^{(m,i)}(x,y,z_{i+1},t) - \sigma_{13}^{(m,i+1)}(x,y,z_{i+1},t) = 0 \quad \text{for} \quad i = 1,\ldots,N_m-1,\ m = 1,\ldots,M \\ &\sigma_{23}^{(1,1)}(x,y,z_1,t) - p_{4b} = 0 \\ &\sigma_{13}^{(1,1)}(x,y,z_1,t) - p_{5b} = 0\end{aligned} \tag{5}$$

These $4N$ algebraic equations can be used to determine the $4N$ unknown constants $\alpha_1^{(m,i)}$, $\beta_1^{(m,i)}$, $\alpha_2^{(m,i)}$, and $\beta_2^{(m,i)}$ $(i = 1, \ldots, N_m,\ m = 1, \ldots, M)$. Here $N(= \sum_{m=1}^{M} N_m)$ is the total number of layers of the laminate. Substituting Eq. (2) and the second equation of Eq. (3) into Eq. (5) we obtain that

$$\{\alpha\} = [A]\{\gamma\} + [B]\begin{Bmatrix} p_{4t} \\ p_{5t} \\ p_{4b} \\ p_{5b} \end{Bmatrix} \tag{6}$$

where $[A]$ is a $4N \times 2M$ constant matrix, $[B]$ is a $4N \times 4$ constant matrix, and

$$\begin{aligned} \{\alpha\} &\equiv \left\{\alpha_1^{(1,1)}, \beta_1^{(1,1)}, \alpha_2^{(1,1)}, \beta_2^{(1,1)}, \ldots, \alpha_1^{(M,N_M)}, \beta_1^{(M,N_M)}, \alpha_2^{(M,N_M)}, \beta_2^{(M,N_M)}\right\}^{\mathrm{T}} \\ \{\gamma\} &\equiv \left\{\gamma_4^{(1)}, \gamma_5^{(1)}, \ldots, \gamma_4^{(M)}, \gamma_5^{(M)}\right\}^{\mathrm{T}} \end{aligned} \tag{7}$$

Because $p_{4t}$, $p_{5t}$, $p_{4b}$, and $p_{5b}$ are usually zero in real applications, they are assumed to be zero in this paper. Hence, one can obtain from Eq. (6) that

$$\begin{aligned} \alpha_1^{(m,i)} &= \sum_{j=1}^{M}\left(a_{14}^{(m,i,j)}\gamma_4^{(j)} + a_{15}^{(m,i,j)}\gamma_5^{(j)}\right) \\ \beta_1^{(m,i)} &= \sum_{j=1}^{M}\left(b_{14}^{(m,i,j)}\gamma_4^{(j)} + b_{15}^{(m,i,j)}\gamma_5^{(j)}\right) \\ \alpha_2^{(m,i)} &= \sum_{j=1}^{M}\left(a_{24}^{(m,i,j)}\gamma_4^{(j)} + a_{25}^{(m,i,j)}\gamma_5^{(j)}\right) \\ \beta_2^{(m,i)} &= \sum_{j=1}^{M}\left(b_{24}^{(m,i,j)}\gamma_4^{(j)} + b_{25}^{(m,i,j)}\gamma_5^{(j)}\right) \end{aligned} \tag{8}$$

where $a_{kl}^{(m,i,j)}$ and $b_{kl}^{(m,i,j)}$ are constants determined by material properties and ply angles. Hence the displacement field of the $i$th layer of the $m$th sublaminate (Eq. (1)) can be presented in the following form:

$$\begin{aligned} u_1^{(m,i)} &= u - w_x z + \gamma_5^{(m)} z + \sum_{j=1}^{M}\left(\gamma_4^{(j)} g_{14}^{(m,i,j)} + \gamma_5^{(j)} g_{15}^{(m,i,j)}\right) \\ u_2^{(m,i)} &= v - w_y z + \gamma_4^{(m)} z + \sum_{j=1}^{M}\left(\gamma_4^{(j)} g_{24}^{(m,i,j)} + \gamma_5^{(j)} g_{25}^{(m,i,j)}\right) \\ u_3^{(m,i)} &= w + \alpha_3^{(m,i)} z + \beta_3^{(m,i)} z^2 \end{aligned} \tag{9}$$

where

$$\begin{aligned} g_{14}^{(m,i,j)} &= a_{14}^{(m,i,j)} z^2 + b_{14}^{(m,i,j)} z^3 \\ g_{15}^{(m,i,j)} &= a_{15}^{(m,i,j)} z^2 + b_{15}^{(m,i,j)} z^3 \\ g_{24}^{(m,i,j)} &= a_{24}^{(m,i,j)} z^2 + b_{24}^{(m,i,j)} z^3 \\ g_{25}^{(m,i,j)} &= a_{25}^{(m,i,j)} z^2 + b_{25}^{(m,i,j)} z^3 \end{aligned} \tag{10}$$

$g_{15}^{(m,i,j)}$ and $g_{24}^{(m,i,j)}$ are called shear warping functions, and $g_{14}^{(m,i,j)}$ and $g_{25}^{(m,i,j)}$ are shear coupling functions. It follows from Eqs. (9) and (2) that the strains are given by

$$
\begin{aligned}
\epsilon_{13}^{(m,i)} &= \gamma_5^{(m)} + \sum_{j=1}^{M} \left( \gamma_4^{(j)} g_{14z}^{(m,i,j)} + \gamma_5^{(j)} g_{15z}^{(m,i,j)} \right) \\
\epsilon_{23}^{(m,i)} &= \gamma_4^{(m)} + \sum_{j=1}^{M} \left( \gamma_4^{(j)} g_{24z}^{(m,i,j)} + \gamma_5^{(j)} g_{25z}^{(m,i,j)} \right) \\
\epsilon_{12}^{(m,i)} &= u_y + v_x - 2z w_{xy} + z\gamma_{5y}^{(m)} + z\gamma_{4x}^{(m)} + \sum_{j=1}^{M} \left( \gamma_{4x}^{(j)} g_{24}^{(m,i,j)} + \gamma_{5x}^{(j)} g_{25}^{(m,i,j)} + \gamma_{4y}^{(j)} g_{14}^{(m,i,j)} + \gamma_{5y}^{(j)} g_{15}^{(m,i,j)} \right) \\
\epsilon_{11}^{(m,i)} &= u_x - z w_{xx} + z\gamma_{5x}^{(m)} + \sum_{j=1}^{M} \left( \gamma_{4x}^{(j)} g_{14}^{(m,i,j)} + \gamma_{5x}^{(j)} g_{15}^{(m,i,j)} \right) \\
\epsilon_{22}^{(m,i)} &= v_y - z w_{yy} + z\gamma_{4y}^{(m)} + \sum_{j=1}^{M} \left( \gamma_{4y}^{(j)} g_{24}^{(m,i,j)} + \gamma_{5y}^{(j)} g_{25}^{(m,i,j)} \right) \\
\epsilon_{33}^{(m,i)} &= \alpha_3^{(m,i)} + 2z\beta_3^{(m,i)}
\end{aligned}
\tag{11}
$$

### 2.2. Transverse normal strain

The transverse normal strain of a laminate is mainly due to external normal loads on the top and bottom surfaces of the laminate and Poisson's effect caused by inplane strains $\epsilon_{11}$, $\epsilon_{22}$, and $\epsilon_{12}$. It follows from the normal stress conditions on the top and bottom surfaces and the continuity conditions of $u_3$ and $\sigma_{33}$ that

$$
\begin{aligned}
&\sigma_{33}^{(M,N_M)}(x,y,z_{N_M+1},t) - p_{3t} = 0 \\
&u_3^{(m,N_m)}(x,y,z_{N_m+1},t) - u_3^{(m+1,1)}(x,y,z_1,t) = 0 \quad \text{for} \quad m = 1,\ldots,M-1 \\
&\sigma_{33}^{(m,N_m)}(x,y,z_{N_m+1},t) - \sigma_{33}^{(m+1,1)}(x,y,z_1,t) = 0 \quad \text{for} \quad m = 1,\ldots,M-1 \\
&u_3^{(m,i)}(x,y,z_{i+1},t) - u_3^{(m,i+1)}(x,y,z_{i+1},t) = 0 \quad \text{for} \quad i = 1,\ldots,N_m-1, \quad m = 1,\ldots,M \\
&\sigma_{33}^{(m,i)}(x,y,z_{i+1},t) - \sigma_{33}^{(m,i+1)}(x,y,z_{i+1},t) = 0 \quad \text{for} \quad i = 1,\ldots,N_m-1, \quad m = 1,\ldots,M \\
&\sigma_{33}^{(1,1)}(x,y,z_1,t) - E_s\left[ Z(t) + w + \alpha_3^{(1,1)} z_1 + \beta_3^{(1,1)} z_1^2 \right] = 0
\end{aligned}
\tag{12}
$$

where $p_{3t}$ denotes the normal stress on the top surface of the laminate, $Z(t)$ is the rigid-body motion of the plate along the $z$-axis, and $E_s$ is the spring constant per unit area of the foundation. If $E_s = 0$ is used, it is equivalent to $\sigma_{33} = 0$. If $E_s = \infty$ is used, it is equivalent to a rigid ground. These $2N$ equations can be used to solve for the $2N$ unknowns $\alpha_3^{(m,i)}$ and $\beta_3^{(m,i)}$ ($i = 1,\ldots,N_m$, $m = 1,\ldots,M$). Substituting the first equation of Eqs. (3) and (11) into Eq. (12) we obtain that

$$
\begin{aligned}
\begin{Bmatrix} \alpha_3^{(m,i)} \\ \beta_3^{(m,i)} \end{Bmatrix} &= \begin{bmatrix} a_{30}^{(m,i)} & a_{31}^{(m,i)} & a_{32}^{(m,i)} \\ b_{30}^{(m,i)} & b_{31}^{(m,i)} & b_{32}^{(m,i)} \end{bmatrix} \begin{Bmatrix} u_x \\ v_y \\ u_y + v_x \end{Bmatrix} + \begin{bmatrix} a_{33}^{(m,i)} & a_{34}^{(m,i)} & a_{35}^{(m,i)} \\ b_{33}^{(m,i)} & b_{34}^{(m,i)} & b_{35}^{(m,i)} \end{bmatrix} \begin{Bmatrix} w_{xx} \\ w_{yy} \\ w_{xy} \end{Bmatrix} \\
&\quad + \sum_{j=1}^{M} \begin{bmatrix} a_{36}^{(m,i,j)} & a_{37}^{(m,i,j)} & a_{38}^{(m,i,j)} & a_{39}^{(m,i,j)} \\ b_{36}^{(m,i,j)} & b_{37}^{(m,i,j)} & b_{38}^{(m,i,j)} & b_{39}^{(m,i,j)} \end{bmatrix} \begin{Bmatrix} \gamma_{4x}^{(j)} \\ \gamma_{4y}^{(j)} \\ \gamma_{5x}^{(j)} \\ \gamma_{5y}^{(j)} \end{Bmatrix} + \begin{bmatrix} a_{41}^{(m,i)} & a_{42}^{(m,i)} & a_{43}^{(m,i)} \\ b_{41}^{(m,i)} & b_{42}^{(m,i)} & b_{43}^{(m,i)} \end{bmatrix} \begin{Bmatrix} p_{3t} \\ w \\ Z \end{Bmatrix}
\end{aligned}
\tag{13}
$$

where $a_{kl}^{(m,i,j)}$, $b_{kl}^{(m,i,j)}$, $a_{pq}^{(m,i)}$, and $b_{pq}^{(m,i)}$ are constants. Hence, we have

$$\epsilon_{33}^{(m,i)} = \{g_{30}, g_{31}, g_{32}, g_{33}, g_{34}, g_{35}\}^{(m,i)}\{\psi_0\} + g_{41}^{(m,i)} p_{3t} + g_{42}^{(m,i)} w + g_{43}^{(m,i)} Z + \sum_{j=1}^{M} \{g_{36}, g_{37}, g_{38}, g_{39}\}^{(m,i,j)} \left\{\psi_1^{(j)}\right\} \tag{14}$$

where

$$\begin{aligned}
\{\psi_0\} &\equiv \{u_x, v_y, u_y + v_x, w_{xx}, w_{yy}, w_{xy}\}^{\mathrm{T}} \\
\left\{\psi_1^{(j)}\right\} &\equiv \left\{\gamma_{4x}^{(j)}, \gamma_{4y}^{(j)}, \gamma_{5x}^{(j)}, \gamma_{5y}^{(j)}\right\}^{\mathrm{T}} \\
g_{3k}^{(m,i)} &\equiv a_{3k}^{(m,i)} + 2z b_{3k}^{(m,i)}, \quad k = 0, 1, \ldots, 5 \\
g_{3k}^{(m,i,j)} &\equiv a_{3k}^{(m,i,j)} + 2z b_{3k}^{(m,i,j)}, \quad k = 6, \ldots, 9 \\
g_{4k}^{(m,i)} &\equiv a_{4k}^{(m,i)} + 2z b_{4k}^{(m,i)}, \quad k = 1, 2, 3
\end{aligned} \tag{15}$$

### 2.3. Stress–strain relation

It follows from Eqs. (11) and (14) that the stress–strain relation can be rewritten as

$$\begin{aligned}
\left\{\sigma^{(m,i)}\right\} &= \left[\overline{Q}^{(m,i)}\right]\left(\left[S_2^{(m,i)}\right]\{\psi_2\} + \sum_{j=1}^{M}\left[S_3^{(m,i,j)}\right]\left\{\psi_3^{(j)}\right\} + \left\{P^{(m,i)}\right\} p_{3t}\right) \\
&= \left[\overline{Q}^{(m,i)}\right]\left(\left[S^{(m,i)}\right]\{\psi\} + \left\{P^{(m,i)}\right\} p_{3t}\right)
\end{aligned} \tag{16}$$

where

$$\begin{aligned}
\left\{\sigma^{(m,i)}\right\} &\equiv \left\{\sigma_{11}^{(m,i)}, \sigma_{22}^{(m,i)}, \sigma_{33}^{(m,i)}, \sigma_{23}^{(m,i)}, \sigma_{13}^{(m,i)}, \sigma_{12}^{(m,i)}\right\}^{\mathrm{T}} \\
\{\psi_2\} &\equiv \{u_x, v_y, u_y + v_x, w_{xx}, w_{yy}, w_{xy}, w, Z\}^{\mathrm{T}} \\
\left\{\psi_3^{(j)}\right\} &\equiv \left\{\gamma_{4x}^{(j)}, \gamma_{4y}^{(j)}, \gamma_{5x}^{(j)}, \gamma_{5y}^{(j)}, \gamma_4^{(j)}, \gamma_5^{(j)}\right\}^{\mathrm{T}} \\
\{\psi\} &\equiv \left\{\{\psi_2\}^{\mathrm{T}}, \left\{\psi_3^{(1)}\right\}^{\mathrm{T}}, \ldots, \left\{\psi_3^{(M)}\right\}^{\mathrm{T}}\right\}^{\mathrm{T}} \\
\left\{P^{(m,i)}\right\} &\equiv \left\{0, 0, g_{41}^{(m,i)}, 0, 0, 0\right\}^{\mathrm{T}} \\
\left[S_2^{(m,i)}\right] &\equiv \begin{bmatrix}
1 & 0 & 0 & -z & 0 & 0 & 0 & 0 \\
0 & 1 & 0 & 0 & -z & 0 & 0 & 0 \\
g_{30} & g_{31} & g_{32} & g_{33} & g_{34} & g_{35} & g_{42} & g_{43} \\
0 & 0 & 0 & 0 & 0 & 0 & 0 & 0 \\
0 & 0 & 0 & 0 & 0 & 0 & 0 & 0 \\
0 & 0 & 1 & 0 & 0 & -2z & 0 & 0
\end{bmatrix}^{(m,i)} \\
\left[S_3^{(m,i,j)}\right] &\equiv \begin{bmatrix}
g_{14} & 0 & z\delta_{mj} + g_{15} & 0 & 0 & 0 \\
0 & z\delta_{mj} + g_{24} & 0 & g_{25} & 0 & 0 \\
g_{36} & g_{37} & g_{38} & g_{39} & 0 & 0 \\
0 & 0 & 0 & 0 & \delta_{mj} + g_{24z} & g_{25z} \\
0 & 0 & 0 & 0 & g_{14z} & \delta_{mj} + g_{15z} \\
z\delta_{mj} + g_{24} & g_{14} & g_{25} & z\delta_{mj} + g_{15} & 0 & 0
\end{bmatrix}^{(m,i,j)}
\end{aligned} \tag{17}$$

where $\delta_{mj}$ is the Kronecker delta function.

## 3. Finite element formulation

The dynamic version of the principle of virtual work states (Washizu, 1982)

$$\int_0^t (\delta K_{\mathrm{E}} - \delta \Pi + \delta W_{\mathrm{nc}})\mathrm{d}t = 0 \tag{18}$$

where $\Pi$ denotes the elastic energy, $K_{\mathrm{E}}$ the kinetic energy, and $W_{\mathrm{nc}}$ the non-conservative energy due to external distributed and/or concentrated loads and dampings.

### 3.1. Elastic energy

It follows from Eq. (16) that

$$\delta \Pi = \sum_{m=1}^{M} \sum_{i=1}^{N_m} \int_A \int_{z_i}^{z_{i+1}} \left\{\delta \epsilon^{(m,i)}\right\}^{\mathrm{T}} \left\{\sigma^{(m,i)}\right\} \mathrm{d}z\, \mathrm{d}A = \int_A \{\delta\psi\}^{\mathrm{T}} ([\Phi]\{\psi\} + \{\hat{\Phi}\} p_{3t})\, \mathrm{d}A \tag{19}$$

where $A$ denotes the area of the reference surface, $N_m$ is the total number of layers of the $m$th sublaminate, and $z_i$ and $z_{i+1}$ indicate the locations of the lower and upper surfaces of the $i$th layer of the $m$th sublaminate. Here we assume that $p_{3t}$ is known and hence $\delta p_{3t} = 0$. Moreover, $[\Phi]$ is a $(6M+8) \times (6M+8)$ symmetric matrix and $\left\{\hat{\Phi}\right\}$ is a $(6M+8) \times 1$ vector given by

$$\begin{aligned} [\Phi] &= \sum_{m=1}^{M} \sum_{i=1}^{N_m} \int_{z_i}^{z_{i+1}} \left[S^{(m,i)}\right]^{\mathrm{T}} \left[\overline{Q}^{(m,i)}\right] \left[S^{(m,i)}\right] \mathrm{d}z \\ \{\hat{\Phi}\} &= \sum_{m=1}^{M} \sum_{i=1}^{N_m} \int_{z_i}^{z_{i+1}} \left[S^{(m,i)}\right]^{\mathrm{T}} \left[\overline{Q}^{(m,i)}\right] \left\{P^{(m,i)}\right\} \mathrm{d}z \end{aligned} \tag{20}$$

Using the finite-element discretization scheme, we discretize the displacements as

$$\left\{u, v, w, \gamma_4^{(1)}, \gamma_5^{(1)}, \ldots, \gamma_4^{(M)}, \gamma_5^{(M)}, Z\right\}^{\mathrm{T}} = [N]\left\{q^{[j]}\right\} \tag{21}$$

where $\left\{q^{[j]}\right\}$ is the displacement vector of the $j$th element and $[N]$ is a matrix of 2-D shape functions. Here four-node rectangular elements are assumed to be used. Each node has $6 + 2M$ DOFs (i.e., $u, v, w$, $w_x, w_y, w_{xy}, \gamma_4^{(1)}, \gamma_5^{(1)}, \ldots, \gamma_4^{(M)}, \gamma_5^{(M)}$) and there is a rigid-body DOF $Z(t)$. Because $Z(t)$ represents the rigid-body motion of the plate, no discretization is needed for $Z(t)$. Hence $[N]$ is a $(2M+4) \times (8M+25)$ matrix. Moreover,

$$\{\psi\} = [D]\left\{q^{[j]}\right\}, \quad [D] \equiv [\partial][N] \tag{22}$$

where $[\partial]$ is a $(6M+8) \times (2M+4)$ matrix consisting of differential operators, and $[D]$ is a $(6M+8) \times (8M+25)$ matrix. Substituting Eq. (22) into Eq. (19) yields

$$\begin{aligned} \delta \Pi &= \sum_{j=1}^{N_{\mathrm{e}}} \int_{A^{[j]}} \left\{\delta q^{[j]}\right\}^{\mathrm{T}} \left([D]^{\mathrm{T}}[\Phi][D]\left\{q^{[j]}\right\} + [D]^{\mathrm{T}}\{\hat{\Phi}\} p_{3t}\right) \mathrm{d}A = \sum_{j=1}^{N_{\mathrm{e}}} \left\{\delta q^{[j]}\right\}^{\mathrm{T}} \left([K^{[j]}]\left\{q^{[j]}\right\} + \left\{f^{[j]}\right\}\right) \\ &= \{\delta q\}^{\mathrm{T}} ([K]\{q\} + \{f\}) \end{aligned} \tag{23}$$

where

$$\left[K^{[j]}\right] \equiv \int_{A^{[j]}} [D]^{\mathrm{T}}[\Phi][D]\,\mathrm{d}A, \qquad \left\{f^{[j]}\right\} = \int_{A^{[j]}} [D]^{\mathrm{T}}\{\hat{\Phi}\}p_{3t}\,\mathrm{d}A \tag{24}$$

$N_{\mathrm{e}}$ is the total number of elements, $A^{[j]}$ is the area of the $j$th element, $[K^{[j]}]$ is the stiffness matrix of the $j$th element, $\{f^{[j]}\}$ is the elemental load vector due to the loading on the top surface, $[K]$ is the structural stiffness matrix, and $\{q\}$ is the structural displacement vector.

We point out here that this finite plate element is a 2-D one but it accounts for 3-D effects caused by interlaminar shear and normal stresses.

### 3.2. Kinetic energy

Because of the initial velocity $V_0$ along the $z$-direction as shown in Fig. 1, the displacement along the $z$-direction consists of two parts. One is $w(x,y,z,t)$ that results in strains, and the other is $Z(t)$ that accounts for the rigid-body motion of the laminate. It follows from Eq. (9) that the total displacements can be re-written as

$$\left\{u^{(m,i)}\right\} = \left[\bar{S}_2^{(m,i)}\right]\left\{\bar{\psi}_2\right\} + \sum_{j=1}^{M}\left[\bar{S}_3^{(m,i,j)}\right]\left\{\bar{\psi}_3^{(j)}\right\} = \left[\bar{S}^{(m,i)}\right]\left\{\bar{\psi}\right\} \tag{25}$$

where

$$\begin{aligned}
&\left\{u^{(m,i)}\right\} \equiv \left\{u_1^{(m,i)}, u_2^{(m,i)}, u_3^{(m,i)} + Z(t)\right\}^{\mathrm{T}}\\
&\{\bar{\psi}_2\} \equiv \{u, v, w, w_x, w_y, Z\}^{\mathrm{T}}\\
&\left\{\bar{\psi}_3^{(j)}\right\} \equiv \left\{\gamma_4^{(j)}, \gamma_5^{(j)}\right\}^{\mathrm{T}}\\
&\{\bar{\psi}\} \equiv \left\{\left\{\bar{\psi}_2\right\}^{\mathrm{T}}, \left\{\bar{\psi}_3^{(1)}\right\}^{\mathrm{T}}, \ldots, \left\{\bar{\psi}_3^{(M)}\right\}^{\mathrm{T}}\right\}^{\mathrm{T}}\\
&\left[\bar{S}_2^{(m,i)}\right] \equiv \begin{bmatrix} 1 & 0 & 0 & -z & 0 & 0\\ 0 & 1 & 0 & 0 & -z & 0\\ 0 & 0 & 1 & 0 & 0 & 1 \end{bmatrix}^{(m,i)}\\
&\left[\bar{S}_3^{(m,i,j)}\right] \equiv \begin{bmatrix} g_{14} & z\delta_{mj} + g_{15}\\ z\delta_{mj} + g_{24} & g_{25}\\ 0 & 0 \end{bmatrix}^{(m,i,j)}
\end{aligned} \tag{26}$$

The kinetic energy due to the change of plate thickness is assumed to be negligible and hence $\alpha_3$ and $\beta_3$ are neglected in Eq. (25). Hence, the variation of kinetic energy is given by

$$\delta K_{\mathrm{E}} = -\sum_{m=1}^{M}\sum_{i=1}^{N_m}\int_A\int_{z_i}^{z_{i+1}}\left\{\delta u^{(m,i)}\right\}^{\mathrm{T}}\rho^{(m,i)}\{\ddot{u}^{(m,i)}\}\,\mathrm{d}z\,\mathrm{d}A = -\int_A\left\{\delta\bar{\psi}\right\}^{\mathrm{T}}\left[\bar{\Phi}\right]\left\{\ddot{\bar{\psi}}\right\}\mathrm{d}A \tag{27}$$

where $\rho^{(m,i)}$ is the mass density of the $i$th layer of the $m$th sublaminate, and $[\bar{\Phi}]$ is a $(6+2M)\times(6+2M)$ symmetric matrix given by

$$[\bar{\Phi}] = \sum_{m=1}^{M}\sum_{i=1}^{N_m}\int_{z_i}^{z_{i+1}}\left[\bar{S}^{(m,i)}\right]^{\mathrm{T}}\rho^{(m,i)}\left[\bar{S}^{(m,i)}\right]\mathrm{d}z \tag{28}$$

Using the same discretization scheme used in Eqs. (21) and (22), we obtain that

$$\{\bar{\psi}\} = [\bar{D}]\{q^{[j]}\}, \quad [\bar{D}] \equiv [\bar{\partial}][\bar{N}] \tag{29}$$

where $[\bar{\partial}]$ is a $(6+2M)\times(4+2M)$ matrix consisting of differential operators, and $[\bar{D}]$ is a $(6+2M)\times(8M+25)$ matrix. Substituting Eq. (29) into Eq. (27) yields

$$\delta K_{\mathrm{E}} = -\sum_{j=1}^{N_{\mathrm{e}}} \int_{A^{[j]}} \{\delta q^{[j]}\}^{\mathrm{T}} [\bar{D}]^{\mathrm{T}} \left[\bar{\Phi}\right] [\bar{D}] \left\{\ddot{q}^{[j]}\right\} \mathrm{d}A = -\sum_{j=1}^{N_{\mathrm{e}}} \{\delta q^{[j]}\}^{\mathrm{T}} \left[M^{[j]}\right] \left\{\ddot{q}^{[j]}\right\} = -\{\delta q\}^{\mathrm{T}} [M] \{\ddot{q}\} \tag{30}$$

where

$$\left[M^{[j]}\right] \equiv \int_{A^{[j]}} [\bar{D}]^{\mathrm{T}} \left[\bar{\Phi}\right] [\bar{D}] \, \mathrm{d}A \tag{31}$$

$[M^{[j]}]$ is the mass matrix of the $j$th element, $[M]$ is the structural mass matrix, and $\{q\}$ is the structural displacement vector.

### 3.3. External loads

The non-conservative virtual work due to external loads is given by

$$\delta W_{\mathrm{nc}} = \int_A \left[ p_{3t} \delta(w + \alpha_3^{(M,N_M)} z_{N_M+1} + \beta_3^{(M,N_M)} z_{N_M+1}^2 + Z) - p_{3b} \delta(w + \alpha_3^{(1,1)} z_1 + \beta_3^{(1,1)} z_1^2 + Z) \right] \mathrm{d}A \tag{32}$$

where the weight of the structure is assumed to be negligible. Moreover, if the external work due to the thickness change is assumed to be negligible and hence $p_{3b} = E_s(w+Z)$, we have

$$\delta W_{\mathrm{nc}} = \int_A [p_{3t} \delta(w+Z) - E_{\mathrm{s}}(w+Z)\delta(w+Z)] \, \mathrm{d}A \tag{33}$$

Here we assume that the plate and foundation keep in contact after their first contact. Discretization yields

$$w + Z = \left\{\hat{N}\right\}^{\mathrm{T}} \{q^{[j]}\} \tag{34}$$

where $\{\hat{N}\}$ is a $1\times(8M+25)$ vector consisting of interpolation functions. Hence, we have

$$\begin{aligned} \delta W_{\mathrm{nc}} &= \sum_{j=1}^{N_{\mathrm{e}}} \int_{A^{[j]}} \{\delta q^{[j]}\}^{\mathrm{T}} \left( \{\hat{N}\} p_{3t} - \{\hat{N}\} E_{\mathrm{s}} \{\hat{N}\}^{\mathrm{T}} \{q^{[j]}\} \right) \mathrm{d}A = \sum_{j=1}^{N_{\mathrm{e}}} \{\delta q^{[j]}\}^{\mathrm{T}} \left( \{F^{[j]}\} - \left[\hat{K}^{[j]}\right] \{q^{[j]}\} \right) \\ &= \{\delta q\}^{\mathrm{T}} (\{F\} - [\hat{K}]\{q\}) \end{aligned} \tag{35}$$

where

$$\left[\hat{K}^{[j]}\right] \equiv \int_{A^{[j]}} \{\hat{N}\} E_{\mathrm{s}} \{\hat{N}\}^{\mathrm{T}} \, \mathrm{d}A, \qquad \{F^{[j]}\} \equiv \int_{A^{[j]}} \{\hat{N}\} p_{3t} \, \mathrm{d}A \tag{36}$$

We note that $\left[\hat{K}^{[j]}\right]$ is an extra stiffness matrix due to the elastic foundation.

### 3.4. Equation of motion

Substituting Eqs. (23), (30), and (35) into Eq. (18) yields the equation of motion as

$$[M]\{\ddot{q}\} + [C]\{\dot{q}\} + ([K] + [\hat{K}])\{q\} = \{F\} - \{f\} \tag{37}$$

where a damping matrix $[C]$ is added.

## 4. Some numerical results and discussions

We consider a 2.44 m × 2.44 m × 3.1 cm sandwich plate consisting of a top face sheet of 48 $AS_4$/3501-6 graphite-epoxy layers, a HRH10-1/8-4.0 Nomax core of 12.7 mm thickness, and a bottom face sheet of 96 $AS_4$/3501-6 layers, as shown in Fig. 1. The plate supports weights from 2225 to 8900 $N$ uniformly distributed over the central half of the upper surface, and the plate is dropped at an initial velocity of 3.05 to 15.24 m/s onto a flat ground surface. The dropping height is assumed to be small and negligible. The ground is sand and is considered to be an isotropic material having an elastic constant $E_s = 67\,864\,000$ N/m$^3$. The material properties of $AS_4$/3501-6 layers are:

$$\begin{aligned}
&E_{11} = 144.8 \text{ GPa}, \quad E_{22} = 9.7 \text{ GPa}, \quad E_{33} = 9.7 \text{ GPa}\\
&v_{12} = 0.3, \quad v_{13} = 0.3, \quad v_{23} = 0.34\\
&G_{12} = 6.0 \text{ GPa}, \quad G_{13} = 6.0 \text{ GPa}, \quad G_{23} = 3.6 \text{ Gpa}\\
&S_{12} = 120.7 \text{ MPa}, \quad S_{13} = 120.7 \text{ MPa}, \quad S_{23} = 89.3 \text{ MPa}\\
&X_t = 2.17 \text{ GPa}, \quad X_c = -1.72 \text{ GPa}, \quad Y_t = 53.8 \text{ MPa}, \quad Y_c = Z_c = -205.5 \text{ MPa}\\
&\text{thickness } \hat{t} = 0.127 \text{ mm}, \quad \text{density} = 1614 \text{ kg/m}^3
\end{aligned} \tag{38}$$

where $E_{ij}$ are Young's moduli, $G_{ij}$ shear moduli, $v_{ij}$ Poisson's ratios, $S_{ij}$ shear failure stresses, $X_t$ the tensile failure stress along the fiber, $X_c$ the compressive failure stress along the fiber, $Y_t$ the tensile failure stress perpendicular to the fiber, and $Y_c$ the compressive failure stress perpendicular to the fiber. The HRH10-1/8-4.0 Nomax honeycomb material has the following material properties:

$$\begin{aligned}
&E_{11} = 80.4 \text{ MPa}, \quad E_{22} = 80.4 \text{ MPa}, \quad E_{33} = 1.005 \text{ GPa}\\
&v_{12} = 0.25, \quad v_{13} = 0.02, \quad v_{23} = 0.02\\
&G_{12} = 32.2 \text{ MPa}, \quad G_{13} = 120.6 \text{ MPa}, \quad G_{23} = 75.8 \text{ GPa}\\
&S_{13} = 177.9 \text{ MPa}, \quad S_{23} = 142.3 \text{ MPa}, \quad Z_c = -3.83 \text{ MPa}\\
&\text{thickness } t_2 = 12.7 \text{ mm}, \quad \text{density} = 139.22 \text{ kg/m}^3
\end{aligned} \tag{39}$$

### 4.1. Shear warping functions

If only one sublaminate is assumed (i.e., $M = m = 1$) and the lamination sequences of the top and bottom laminates are $[0^\circ_{48}]$ and $[0^\circ_{96}]$, respectively, the sandwich plate is an orthotropic laminate and hence there is no shear couplings, i.e., $g_{14}^{(m,i,j)} = g_{25}^{(m,i,j)} = 0$ in Eq. (9). Consequently, it follows from Eq. (9) that the transverse shear warpings $W_1(z)$ and $W_2(z)$ are given by

$$W_1 \equiv z + g_{15}^{(1,i,1)}, \qquad W_2 \equiv z + g_{24}^{(1,i,1)} \tag{40}$$

And, it follows from Eq. (11) that

$$\epsilon_{13}^{(1,i)}/\gamma_5^{(1)} = W_{1z}, \qquad \epsilon_{23}^{(1,i)}/\gamma_4^{(1)} = W_{2z} \tag{41}$$

Fig. 3(a) and (b) show the shear warping functions, and Fig. 3(c) and (d) show the distributions of transverse shear strains. We note that the two shear warping functions are different, and $W_1$ is significantly different from the shear warping function of isotropic plates. Fig. 3(c) and (d) show that the Nomax core has larger shear deformations than the two face sheets. Because of orthotropy, $\overline{Q}_{45}^{(m,i)} = 0$ in Eq. (4). Hence, it follows from Eqs. (3), (4) and (41) that

$$\sigma_{13}^{(1,i)}/\gamma_5^{(1)} = \overline{Q}_{55}^{(1,i)} W_{1z}, \qquad \sigma_{23}^{(1,i)}/\gamma_4^{(1)} = \overline{Q}_{44}^{(1,i)} W_{2z} \tag{42}$$

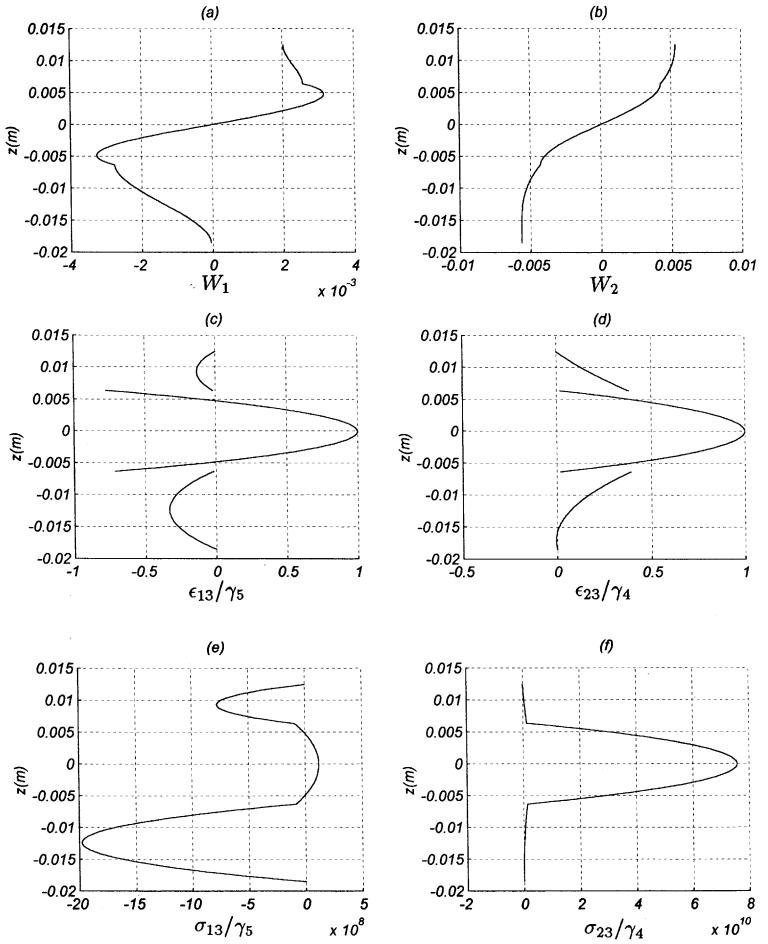


Fig. 3. Transverse shear warpings of the $[0^\circ_{96}/\text{core}/0^\circ_{48}]$ sandwich plate using one sublaminate: (a) $W_1$, (b) $W_2$, (c) $\epsilon_{13}/\gamma_5$, (d) $\epsilon_{23}/\gamma_4$, (e) $\sigma_{13}/\gamma_5$, and (f) $\sigma_{23}/\gamma_4$.

Fig. 3(e) and (f) show the distributions and continuity of transverse shear stresses. We note that the assumed lamination sequence results in a large $\sigma_{23}$ in the core and a large $\sigma_{13}$ in the face sheets.

If three sublaminates (i.e., $M = 3$) are used in modeling the $[0^\circ_{96}/\text{core}/0^\circ_{48}]$ sandwich plate with the bottom face sheet as the first sublaminate, the Nomax core as the second sublaminate, and the top face sheet as the third sublaminate, it follows from Eq. (9) that the shear warpings are given by

$$\begin{aligned}
u_1^{(1,i)} - u + w_x z &= \gamma_5^{(1)}\left(z + g_{15}^{(1,i,1)}\right) + \gamma_5^{(2)} g_{15}^{(1,i,2)} + \gamma_5^{(3)} g_{15}^{(1,i,3)} \\
u_1^{(2,i)} - u + w_x z &= \gamma_5^{(1)} g_{15}^{(2,i,1)} + \gamma_5^{(2)}\left(z + g_{15}^{(2,i,2)}\right) + \gamma_5^{(3)} g_{15}^{(2,i,3)} \\
u_1^{(3,i)} - u + w_x z &= \gamma_5^{(1)} g_{15}^{(3,i,1)} + \gamma_5^{(2)} g_{15}^{(3,i,2)} + \gamma_5^{(3)}\left(z + g_{15}^{(3,i,3)}\right)
\end{aligned} \tag{43}$$

Fig. 4(a)–(c) show the shear warpings $W_{11}$, $W_{12}$, and $W_{13}$ corresponding to $\gamma_5^{(1)}$, $\gamma_5^{(2)}$, and $\gamma_5^{(3)}$, respectively. If $\gamma_5^{(1)} = \gamma_5^{(2)} = \gamma_5^{(3)}$ is assumed in Eq. (43), Fig. 4(d) shows the distribution of $(u_1^{(m,i)} - u + w_x z)/\gamma_5^{(1)}$, which is the same as Fig. 3(a). If $10\gamma_5^{(1)} = \gamma_5^{(2)} = 10\gamma_5^{(3)}$ is assumed in Eq. (43), Fig. 4(e) shows the distribution of

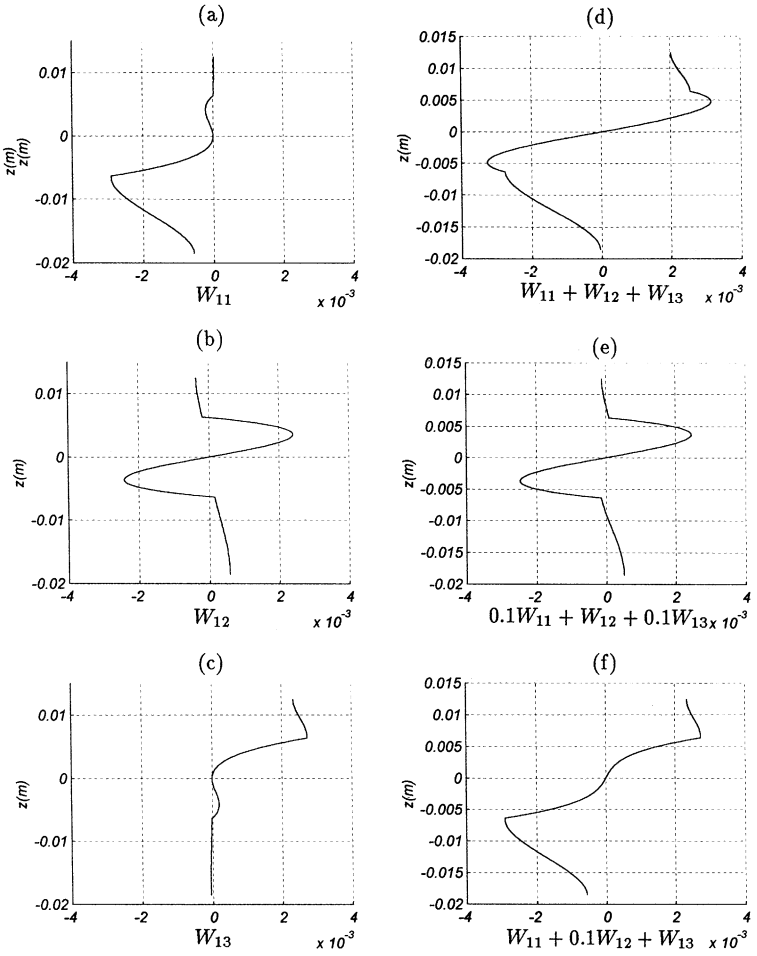


Fig. 4. Transverse shear warpings of the $[0^\circ_{96}/\text{core}/0^\circ_{48}]$ sandwich plate using three sublaminates: (a) $W_{11}$, (b) $W_{12}$, (c) $W_{13}$, (d) $W_{11} + W_{12} + W_{13}$, (e) $0.1W_{11} + W_{12} + 0.1W_{13}$, and (f) $W_{11} + 0.1W_{12} + W_{13}$.

$(u_1^{(m,i)} - u + w_x z)/\gamma_5^{(2)}$. Moreover, if $\gamma_5^{(1)} = 10\gamma_5^{(2)} = \gamma_5^{(3)}$ is assumed in Eq. (43), Fig. 4(f) shows the distribution of $(u_1^{(m,i)} - u + w_x z)/\gamma_5^{(1)}$. The shear warping functions shown in Fig. 4(d)–(f) are very different, but each one of them has a continuous $\sigma_{13}$ because each one of $W_{1i}$ has a continuous $\sigma_{13}$. It has been shown in the literature that the shapes of shear warping functions may vary with the spatial location, vibration frequency, loading and boundary conditions, and structural dimensions (Savoia and Reddy, 1992; Renton, 1991). Because the actual warping functions depend on the ratio $\gamma_5^{(1)}$:$\gamma_5^{(2)}$:$\gamma_5^{(1)}$ and $\gamma_5^{(i)}$ are determined by loading and boundary conditions, the actual warping functions become deformation-dependent. In other words, the use of sublaminates and hence more dependent variables enables the modeling of shear warping functions that change with the spatiallocation, vibration frequency, loading and boundary conditions, and structural dimensions. If each layer is treated as a sublaminate, the number of dependent variables will be $3 + 2N$ (i.e., $u,v,w,\gamma_4^{(1)},\gamma_5^{(1)},\ldots,\gamma_4^{(N)},\gamma_5^{(N)}$) and the theory is equivalent to that of Barbero et al. (1990).

If the sandwich plate is not an orthotropic laminate, shear coupling functions $g_{14}$ and $g_{25}$ exist and hence the distributions of $\epsilon_{13}$ and $\epsilon_{23}$ depend on the values of $\gamma_4$ and $\gamma_5$, which are determined by loading and boundary conditions. For example, if the lamination of the sandwich plate is $[-45^\circ_{96}/\text{core}/45^\circ_{48}]$ and $M = 1$

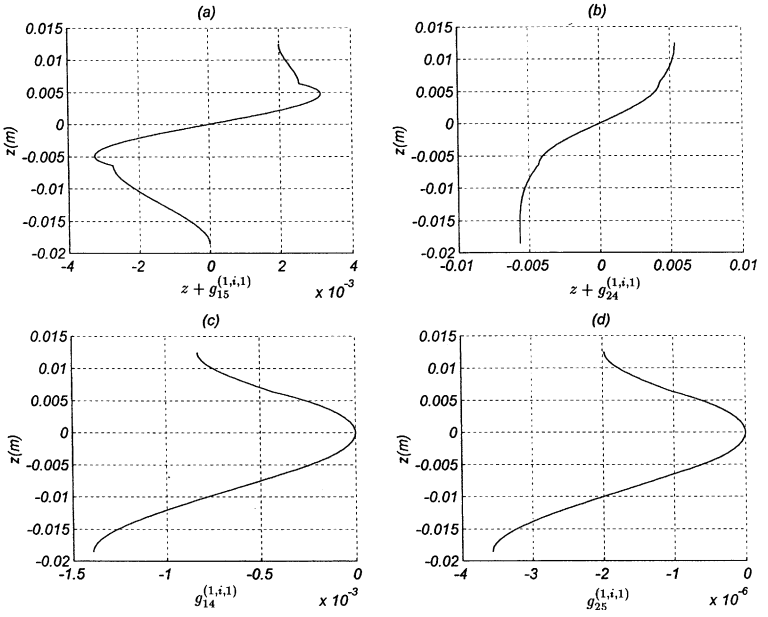


Fig. 5. Shear warping and coupling functions of the $[-45^\circ_{96}/\text{core}/45^\circ_{48}]$ sandwich plate using one sublaminate: (a) $z + g_{15}^{(1,i,1)}$, (b) $z + g_{24}^{(1,i,1)}$, (c) $g_{14}^{(1,i,1)}$, and (d) $g_{25}^{(1,i,1)}$.

is used, Fig. 5 shows the shear warping functions $z + g_{15}^{(1,i,1)}$ and $z + g_{24}^{(1,i,1)}$ and the shear coupling functions $g_{14}^{(1,i,1)}$ and $g_{25}^{(1,i,1)}$. If the lamination of the sandwich plate is $[0^\circ_{24}/30^\circ_{48}/0^\circ_{24}/\text{core}/0^\circ_{12}/60^\circ_{24}/0^\circ_{12}]$ and $M = 1$ is used, Fig. 6 shows the shear warping functions and shear coupling functions. We note that shear coupling functions are significantly changed by the stacking sequence.

### 4.2. Transverse normal strain

The transverse normal strain $\epsilon_{33}$ is induced by external normal loads and Poisson's effect due to in-plane strains. It follows from Eq. (14) that $g_{30}$ represents the transverse normal strain caused by the inplane extensional strain $u_x$, $g_{31}$ is caused by the in-plane extensional strain $v_y$, $g_{32}$ is caused by the in-plane shear strain $u_y + v_x$, $g_{33}$ is caused by the bending curvature $w_{xx}$, $g_{34}$ is caused by the bending curvature $w_{yy}$, $g_{35}$ is caused by the twisting curvature $w_{xy}$, $g_{41}$ is caused by the external load $p_{3t}$, $g_{42}$ is caused by the deformation $w$ against the foundation, $g_{43}$ is caused by the rigid-body movement $Z$ against the foundation, and $g_{36}$, $g_{37}$, $g_{38}$, and $g_{39}$ are due to the variations of $\gamma_4$ and $\gamma_5$ across the reference plane. Eq. (15) shows that these functions are linear functions of $z$. For the $[0^\circ_{96}/\text{core}/0^\circ_{48}]$ sandwich plate, Fig. 7 shows some of the transverse normal strain functions. Because this laminate is orthotropic, $g_{32} = g_{35} = g_{36} = g_{39} = 0$ and $g_{42} = g_{43}$. We note that, although $g_{41}$ (caused by $p_{3t}$) is smaller than others, $p_{3t}$ can have a value much larger than others because it has a different unit.

For the $[0^\circ_{24}/30^\circ_{48}/0^\circ_{24}/\text{core}/0^\circ_{12}/60^\circ_{24}/0^\circ_{12}]$ sandwich plate, Fig. 8 shows the normal strain functions. Again, $g_{42} = g_{43}$. However, because of anisotropy, $g_{32}$, $g_{35}$, $g_{36}$, and $g_{39}$ are non-trivial.

### 4.3. Discussions

For any sandwich plate with a specific stacking sequence, one can obtain its shear warping functions and normal strain functions by following the same procedures shown in Sections 4.1 and 4.2. After the $u$, $v$, $w$,

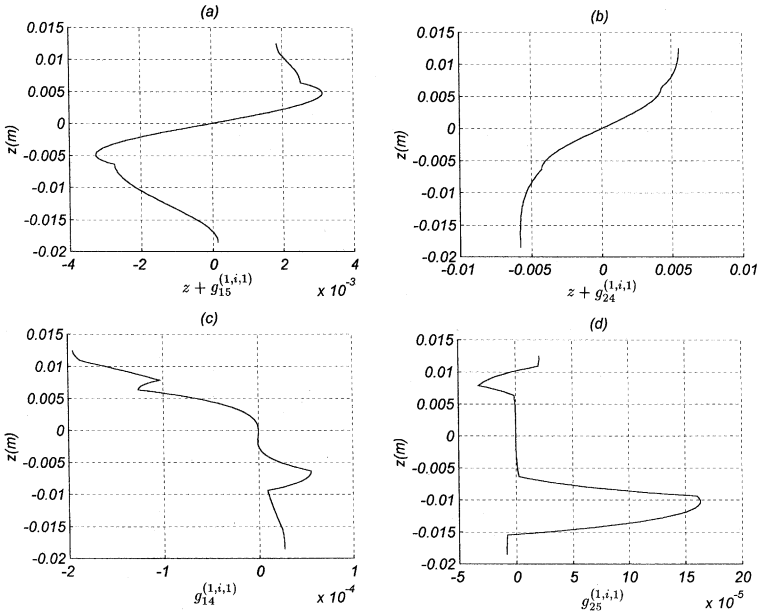


Fig. 6. Shear warping and coupling functions of the $[0^\circ_{24}/30^\circ_{48}/0^\circ_{24}/\text{core}/0^\circ_{12}/60^\circ_{24}/0^\circ_{12}]$ sandwich plate using one sublaminate: (a) $z + g_{15}^{(1,i,1)}$, (b) $z + g_{24}^{(1,i,1)}$, (c) $g_{14}^{(1,i,1)}$, and (d) $g_{25}^{(1,i,1)}$.

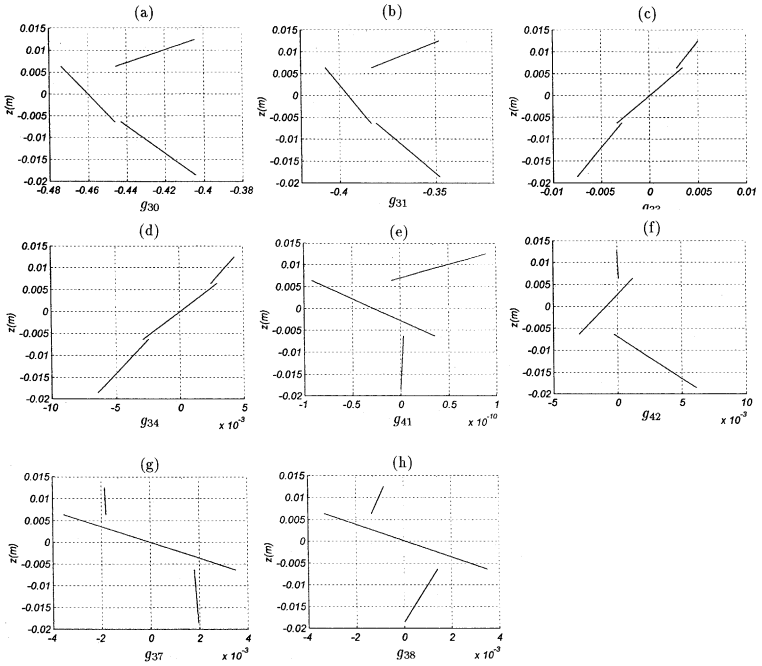


Fig. 7. The normal strain functions of the $[0^\circ_{96}/\text{core}/0^\circ_{48}]$ sandwich plate using one sublaminate: (a) $g_{30}$, (b) $g_{31}$, (c) $g_{33}$, (d) $g_{34}$, (e) $g_{41}$, (f) $g_{42}$, (g) $g_{37}$, and (h) $g_{38}$.

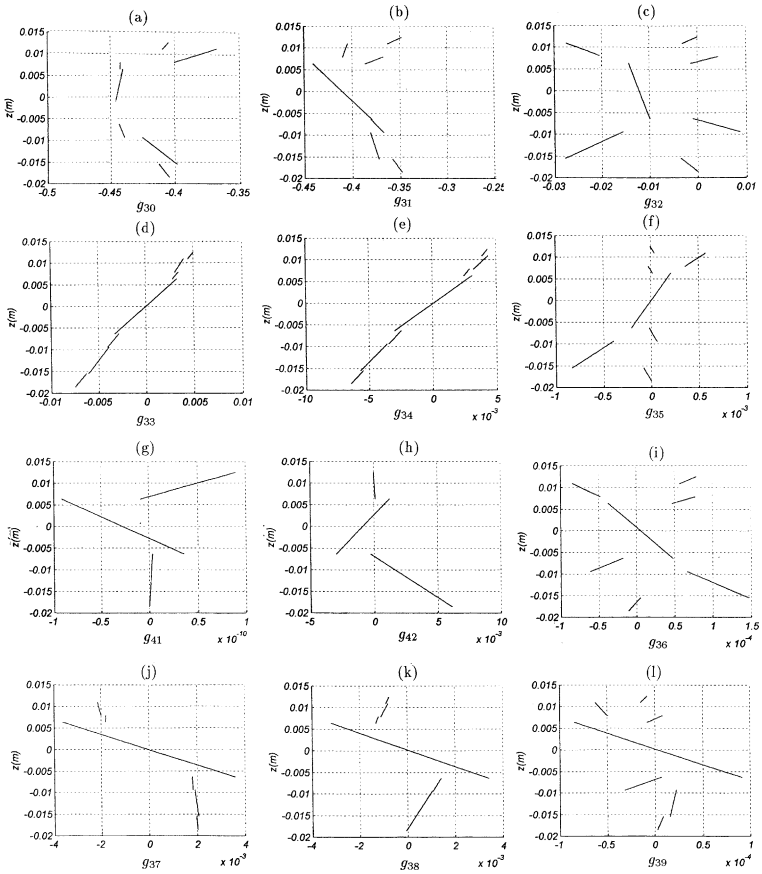


Fig. 8. The normal strain functions of the $[0^\circ_{24}/30^\circ_{48}/0^\circ_{24}/\text{core}/0^\circ_{12}/60^\circ_{24}/0^\circ_{12}]$ sandwich plate using one sublaminate: (a) $g_{30}$, (b) $g_{31}$, (c) $g_{32}$, (d) $g_{33}$, (e) $g_{34}$, (f) $g_{35}$, (g) $g_{41}$, (h) $g_{42}$, (i) $g_{36}$, (j) $g_{37}$, (k) $g_{38}$, and (l) $g_{39}$.

$\gamma_4^{(i)}$, and $\gamma_5^{(i)}$ are obtained by solving the whole structural problem with specified loading and boundary conditions, one can use Eqs. (11) and (14) to obtain the distributions of strains, and use Eqs. (3) and (4) to obtain stresses.

Transient dynamic analysis using the derived finite element model (Eq. (37)), predictions of the initiation and location of critical matrix crack and the threshold of impact damage using Hashin's criterion (Hashin, 1980), and modeling and dynamics of the sandwich plate with cracks will be reported separately.

## 5. Concluding remarks

We presented a 2-D sandwich plate theory that can account for layerwise higher-order transverse shear strains, transverse normal stress, continuity of interlaminar shear and normal stresses, normal stresses on the top and bottom surfaces, free shear-stress conditions on the bonding surfaces, and deformation dependency of shear warpings. The derived shear strain functions show interesting shear coupling effects, and the normal strain functions show thickness change due to external normal loads and Poisson's effect.

## Acknowledgements

This work is supported by the Air Force Office of Scientific Research with Dr. Steven Walker as the technical monitor, the University of Missouri Research Board, and the National Science Foundation through Grant CMS-9912482. The support is gratefully acknowledged.

## References

Barbero, E.J., Reddy, J.N., Teply, J.L., 1990. An accurate determination of stresses in thick laminates using a generalized plate theory. Int. J. Numer. Meth. Engng. 29, 1–14.

Bhimaraddi, A., 1995. Sandwich beam theory and the analysis of constrained layer damping. J. Sound Vibr. 179 (4), 591–602.

Choi, H.Y., Downs, R.J., Chang, F.K., 1991. A new approach toward understanding damage mechanisms and mechanics of laminated composites due to low-velocity impact: Part I – experiments. J. Compos. Mater. 25, 992–1011.

Harrington, T.M., 1994. An Experimental Investigation of Sandwich Panels under Low Velocity Impact. MS Thesis, Air Force Institute of Technology, Wright-Patterson AFB, Ohio.

Hashin, Z., 1980. Failure criteria for unidirectional fiber composites. J. Appl. Mech. 47, 329–334.

Pai, P.F., 1995. A new look at shear correction factors and warping functions of anisotropic laminates. Int. J. Solids Struct. 32, 2295–2313.

Pai, P.F., Nayfeh, A.H., Oh, K., Mook, D.T., 1993. A refined nonlinear model of composite plates with integrated piezoelectric actuators and sensors. Int. J. Solids Struct. 30, 1603–1630.

Pai, P.F., Palazotto, A.N., 1995. Nonlinear displacement-based finite- element analyses of composite shells – a new total Lagrangian formulation. Int. J. Solids Struct. 32, 3047–3073.

Renton, J.D., 1991. Generalized beam theory applied to shear stiffness. Int. J. Solids Struct. 27, 1955–1967.

Savoia, M., Reddy, J.N., 1992. A variational approach to three-dimensional elasticity solutions of laminated composite plates. J. Appl. Mech. 59, 166–175.

Shames, I.H., Dym, C.L., 1985. Energy and Finite Element Methods in Structural Mechanics. McGraw-Hill, New York.

Washizu, K., 1982. Variational Methods in Elasticity and Plasticity. Third edition, Pergamon Press, New York.

Whitney, J.M., 1987. Structural Analysis of Laminated Anisotropic Plates. Technomic Publishing, Lancaster, PA.